A Robust guideline to design a split gradient coil for a hybrid Linac-MRI scanner

Hector Sanchez-Lopez[1], Fangfang Tang[1], and Stuart Crozier[1]
[1]*School of Information Technology & electrical Engineering, The University of Queensland, Brisbane, QLD, Australia*

Target Audience: This work will be of interest of those interested in the design of gradient coils for conventional and hybrid MRI scanners.

Purpose: This study aims to determine the optimal shielding strategy for a 500 mm transversal and 620 mm axial gap split x-gradient coil to be installed in a hybrid Linac-MRI scanner. Two previous studies have presented the challenges to overcome when increasing the gap in split gradient coils [1,2], these include: low efficiency (gradient strength/current), poor shielding ratio $max(B_z^{eddy}/ B_z^{coil})_{DSV}$, mechanically intolerable net torques around 700 Nm (unbalanced coils), regions of very high current density leading to wire width tracks around 1 mm or less, patterns of high manufacturing difficulties due to excessive reversing turns and high coupling with the surrounding structures leading to increased boil-off of helium and possible quenching. These and other challenges are usually encountered by coil manufacturers and developers when facing the necessity of splitting a transverse gradient coil. In this study we have established a robust design methodology to effectively mitigate some of the characteristic shortcomings presented in the design of split coils. We hypothesize that by determining the optimal shielding strategy and further balancing the coil per half it is possible to find solutions capable of producing 20 mT/m using a 600 A amplifier and yet fulfill shielding and manufacturing requirements of a modern hybrid scanner. This study is divided in two parts: studying the shielding strategy and balancing the split gradient coil.

Methods: Four active shielding approaches were implemented in the EMC code [3] and 18 coils were designed for each strategy. The shielding ratio was varied from 0.2% to 2% in order to observe the behavior of following parameters: slew rate, torque, maximum current density, magnetic field flux density and average power loss in the cryostat, stored magnetic energy and secondary field deviation from primary field when the current is driven at 1 kHz. The cold shield cryostat made of aluminum was included in the design process; a uniform gradient field of 10 mT/m was specified in a 300 mm DSV with 5 % of maximum deviation from the target field for all the designs. The stream function was discretized using 20 contours and a constant wire track width and a minimum gap between tracks were set to 8 mm and 3 mm, respectively. The coil envelope is defined as folded structure with mean primary and secondary surface radius at 310 mm and 407 mm respectively. The inner and outer axial positions were set to 270 mm and 950 mm, respectively. In order to assure the repeatability of the experiment we assumed at this stage that the coil is embedded in a 1 T uniform static magnetic field.

a

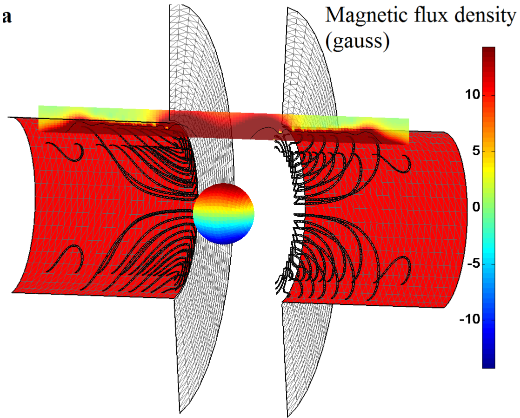

In **option 1**, the field produced by the current induced in the cryostat is constrained to be linear in the same direction as that produced by the coil in the DSV; at the same time the shielding ratio is constrained to a small value in the range 0.2% to 2%. In **option 2** (classic shielding Bz constrained at the cold shield), the normal component of the field produced by the coil is constrained to small value in the cryostat such that the shielding ratio is in the specified range. In **option 3** the total power loss in the whole system is minimized and in **option 4** the total stored energy is minimized in the whole system such that the shielding ratio lies on the target range. The coils were not torque balanced yet as it conflicts with the observed parameters.

Results: Figure a) shows the cold shield, the DSV and one of the coils designed in this study. Figures b)-h) describe the behavior of the parameters observed during the experiment when the shielding ratio increases from 0.2% (super-shield) to 2% (shield). The coil can be considered nearly unshielded if the shielding ratio is much larger than 10%. The net torque corresponds to only a half of the coil.

Discussions: Figure b) shows that option 1 tends to produce the smallest slew rate when super-shield is required. This is due to hard constrains imposed to the coil and the current induced in the cryostat, which must be arranged such that the field is constrained in the DSV to nearly zero but at the same time linear. Therefore, coils design under this option strategy suffers from high current density hence manufacturing difficulties. The slew rate for coil designed under options 3 and 4 tend tends to slightly increase as the coil become less shielded. Figure c) demonstrates that coil designed under **option 3 and 4 are more suitable for torque balanced than that designed using classic shielding and option 1.** Figure d) clearly indicates that **larger wire spreading is obtained when the total minimization of the stored energy is required**. **Classic shielding is not recommended if lower power loss is demanded** in the coil pattern. Figure e) shows that a low field in the cryostat is produced by those coils where the field is constrained to small values however it doesn't means that the power loss or stored energy in the cryostat is the smallest. Around 30 gauss in the cryostat produces a shielding ratio within the range 0.2% to 2%. Figure f) describes that when the power minimization in the cryostat is a priority **the recommended shielding strategies are 3 and 4**, respectively. Classic shielding produce coils where the power loss in the cryostat is close to that generated by coil designed with options 3 or 4. When the secondary field is constrained to be as linear as the primary field (Option 1), the shield coil allows leaking field in the cryostat (figure e); with severe consequences on the power loss and the stored energy (figure g). Figure h) show that coils designed using the **classic shielding approach may lead to a complex and unpredictable spatiotemporal behavior of the secondary field hence a poor pre-emphasis outcome**. Option 1 produce coils for optimal pre-emphasis as the primary and secondary fields match but in detriment of coil performance.

b

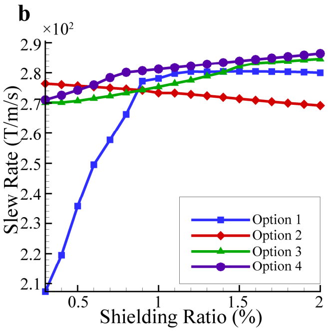

c

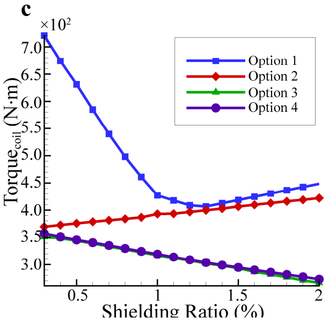

d

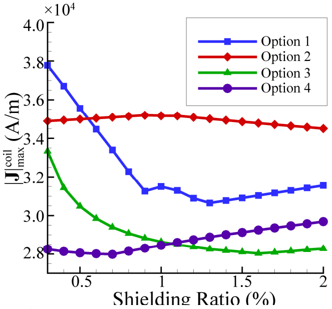

e

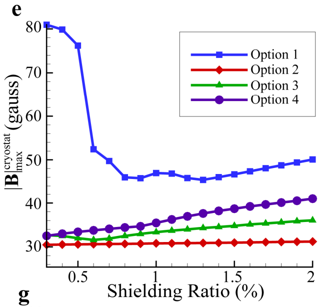

f

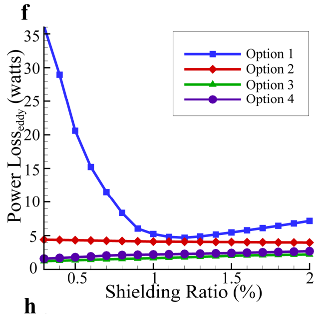

g

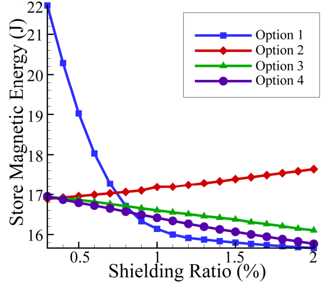

h

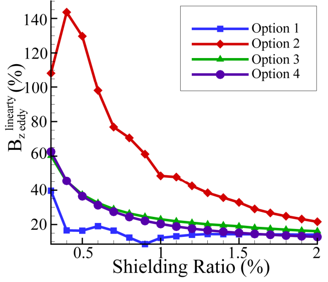

Conclusions: This study present the first part of a complete and robust guideline to design split gradient coils with a large bore and 500 mm central gap. The approach starts with the optimal shielding criteria (this work) and ends with torque/force balancing using an optimal shielding. 1-The minimization of the stored magnetic energy in the whole system leads to coil with high slew rates, suitable coils for torque balancing, minimal current density hence, low power loss in the coil and cryostat and optimal pre-emphasis. 2-Clasic shielding option leads to coils with high current density thus possible high power loss, and unpredictable spatiotemporal behavior of the secondary field hence poor eddy current compensation. 3-The shielding option 2 (coil designed for optimal pre-emphasis) leads toward coils with highly unbalanced torque up to 700 Nm and high power loss in the cryostat.

References:[1] L. Liu, et al, J Magn Reson. vol. 226, pp. 70-78, 2013. [2] L. Liu, et al, J Magn Reson. vol. 222, pp. 8-15, 2012. [2] H. Sanchez, et al J Magn Reson, 199, 48-55, (2009)